Proton and pion structure functions in the improved valon model

H. W. Kua,* L. C. Kwek, and C. H. Oh†
Faculty of Science, Department of Physics, National University of Singapore, Lower Kent Ridge Road, Singapore 119260, Republic of Singapore

(Received 17 February 1998; revised manuscript received 5 August 1998; published 10 March 1999)

The proton structure functions and their moments, at low Q^2, and pion structure functions are derived and analyzed in an improved version of the valon model. Proton structure functions are compared with experiment data from deep inelastic scattering while pion structure functions are compared to Drell-Yan scattering where the invariant mass of the produced muon pairs falls in the range $4.05<m_{\mu\mu}<8.55$ GeV/c^2 at a fixed Q^2 of 25 $(\mathrm{GeV}/c^2)^2$. The first two moments for the pion valence structure function at $Q^2=49$ $(\mathrm{GeV}/c^2)^2$ are also compared with the results from the other models and experimental data. We conclude that this simple, improved physical picture is relevant as far as the presently attainable experimental data are concerned. [S0556-2821(99)03907-7]

PACS number(s): 13.88.+e, 12.39.−x, 13.60.Hb, 14.20.Dh

I. INTRODUCTION

The idea of quark cluster is not a new one. Indeed, this idea has been used in the context of a broken $SU(6)_W \times O(3)$ [1]. However, in the valon model, the hadron is envisaged as a bound state of valence quark clusters called valons [2,3]. For example, the bound state of π^- consists of a ''anti-up'' and a ''down'' valon. These valons thus bear the quantum numbers of the respective valence quarks. It is worth noting that this view can be reconciled with the popular description of hadron structure in terms of partons since these partons can be considered as the components of valons which can be ''observed'' at higher resolutions of the valons. Moreover, the valon can be often considered as a ''dressed'' valence quark. By assuming the formation of valons as valence quarks undergo Q^2 evolutions in QCD and providing a representation for the hadronic wave function in terms of the valons, Hwa [2] found evidence in the deep inelastic neutrino scattering data that suggested their existence. Hwa [3] had also successfully formulated a treatment of the low-p_T reactions based on the structural analysis of the valons. Hwa and Zahir [4] applied the model to determine the flavor-dependent valon distributions in the nucleons which could be used as the solution of the bound-state problem. They also inferred the difference between the matter-density and charge-density distributions, which touches on an important issue mentioned in Ref. [5]. The derived parton distributions and nucleon structure functions, with virtually no arbitrary assumptions or parameters except in the specification of the number of relevant flavors, also agreed with experimental results at high-Q^2 momentum transfer. Arash [6] has recently applied the valon model to study the contributions of the constituents of the proton to its spin in deep inelastic scattering (DIS). Results of the model calculation agree well with the European Muon Collaboration (EMC) results [7]. However, despite the success of the valon model for investigating the structure functions of nucleons, it has not hitherto been applied to the study of the pion.

Unlike the case of nucleons, where data can be obtained from DIS, experimental data for the structure of pions can only be obtained from the Drell-Yan process in which the scattering between a nucleon and a pion produces a lepton pair from the electromagnetic annihilation of a quark and antiquark pairs in the colliding hadrons. Data from DIS processes for pions will only be available after 1998.[1]

In this paper, we investigate the low-Q^2 behavior of the structure functions of the proton using an improved valon model and apply the model to the study of the pion from the Drell-Yan data. Improvements we have made to the original valon model are presented in Sec. II. In order to reconstruct the structure functions from the moments, the inverse Mellin transform is discussed in Sec. III. In Sec. IV, the moments of the structure functions of proton at low Q^2 are derived from the improved valon model and the structure functions are retrieved through the inverse Mellin transform. Derivations of the π^- total and valence structure function moments are presented in Secs. V and VI, respectively. The valon distribution functions of π^- are derived in Sec. VII and fitting to the experimental Drell-Yan scattering data and comparison of the first two moments with other sources are carried out in Sec. VIII. In Sec. IX, we examine the scale-breaking property of our improved valon model. We reiterate the main points in the final section.

II. IMPROVED VALON MODEL

Partons in the valons are classified either as favored, G_f, or unfavored, G_{uf}, distribution functions in Ref. [4]. Although this picture works in the realm of high Q^2, that is, high probing energy, in deep inelastic scattering, we need to modify this notion when the probing energy is low. Physically, the ability to associate partons in the concerned valons as favored or unfavored distribution depends heavily on how much we can ''observe'' and ''identify'' the types of par-

*Email address: scip6073@leonis.nus.edu.sg
†Email address: phyohch@nus.edu.sg

[1]Through private communications with Gerrit Schierholz, Desy.

tons. The favored distribution G_f describes the structure function of a quark within a valon of the same flavor while the unfavored distribution G_{uf} describes the structure function of any flavor or quark of a different flavor in the valon. In deep inelastic scattering where the probing energy is high, one can resolve the quarks residing within the nucleon. In this way, it is plausible to identify favored and unfavored distributions. With low probing energies, this identification is not possible and we need to associate a probability with our interpretation of what we ''see'' as behaving as a favored or unfavored distribution.

For processes that are essentially not DIS in nature, for instance, Drell-Yan scattering, one needs to take on this probabilistic approach in the classification of favored and unfavored distributions. This method is reminiscent of a similar modification in particle production mechanisms in which one can provide a good description of multiparticle production at 900 GeV by replacing the negative binomial distribution (NBD) with a sum of two different NBDs using a relative weight between them [8].

In the case of the valon model, this implies the following mathematical changes to the original valon equations:

$$G_f \rightarrow pG_f + (1-p)G_{uf},$$
$$G_{uf} \rightarrow qG_{uf} + (1-q)G_f, \tag{1}$$

where p and q are the probabilities or weights associated with the respective parton distribution function. These probabilities or weights should approach unity when Q^2 is high, thus reducing to the original valon model [4].

III. RECONSTRUCTION OF STRUCTURE FUNCTION FROM MOMENTS

While it is relatively easy to compute the nth moment from the structure functions, the inverse process is not obvious. To do this inversion, we adopt a mathematically rigorous and easy method [9] by Yndurain to invert the moments and retrieve the structure functions. We define the moments as

$$\mu_n(Q^2) = \int_0^1 F_2(x,Q^2)x^n dx = M(n+2,Q^2), \tag{2}$$

where n is the order of the moment.

As a basis, we have chosen the normalized Bernstein polynomial [11,12]

$$b^{N,k}(x) = \frac{(N+1)!}{k!}\sum_{l=0}^{N-k}\frac{(-1)^l}{l!(N-k-l)!}x^{k+l}, \tag{3}$$

where $k=0,1,\ldots,N$, as a weighting function over x, the fraction of the total proton momentum carried by the partons. We introduce $x_{N,k}$, the weighted x, defined as

$$x_{N,k} = \int_0^1 b^{(N,k)}(x)x\,dx = \frac{k+1}{N+2} \tag{4}$$

and an averaged structure function F_2 around $x_{N,k}$ defined as

$$\tilde{F}_2(x_{N,k}) = \int_0^1 b^{(N,k)}(x)F_2(x)dx. \tag{5}$$

Using Eq. (3), the above expression becomes

$$\tilde{F}_2(x_{N,k}) = \frac{(N+1)!}{k!}\sum_{l=0}^{N-k}\frac{(-1)^l}{l!(N-k-l)!}\mu_{k+l}(Q^2)$$
$$= \frac{(N+1)!}{k!}\sum_{l=0}^{N-k}\frac{(-1)^l}{l!(N-k-l)!}M(k+l+2,Q^2). \tag{6}$$

Moreover, as shown in Ref. [9], the structure function $F_2(x_{N,k})$ is related to the averaged structure function $\tilde{F}_2(x_{N,k})$ using the relation

$$F_2(x_{N,k}) = \tilde{F}_2(x_{N,k}) + \delta(x_{N,k}), \tag{7}$$

where

$$\delta(x_{N,k}) = \frac{1}{2}\frac{(N+1)!(N-k+1)}{k!(N+2)^2(N+3)}$$
$$\times\sum_{l=0}^{N-k}\frac{(-1)^l(k+l)(k+l-1)}{l!(N-k-l)!}\mu_{k+l-2}. \tag{8}$$

Thus, using Eqs. (6) and (7), one can always invert the moments and obtain the averaged structure function $\tilde{F}_2(x_{N,k})$ and structure function $F_2(x_{N,k})$, respectively.

IV. PROTON STRUCTURE FUNCTION AT LOW Q^2

Let $F^P(x,Q^2)$ be the structure function of the proton, $F^\nu(z,Q^2)$ be the corresponding function of a valon ν, and $G_{\nu/P}(y)$ be the probability that a valon ν has momentum fraction y in the proton. Then,

$$F^P(x,Q^2) = \sum_\nu^3 \int_x^1 G_{\nu/P}(y)F^\nu\left(\frac{x}{y},Q^2\right)\frac{dy}{y}, \tag{9}$$

where the summation is taken over the three valons present in the nucleon.

In expression (9), we have assumed the following: (i) the three valons carry all the momentum of the proton; (ii) at the higher energies, the valons are independently probed, which is reasonable considering the shortness of interaction time; (iii) the internal structure of the valon in this model cannot be resolved at Q_0. As such, we expect that $F^P(z,Q^2)$ becomes $\delta(z-1)$ as Q is extrapolated to Q_0 [10]. As in Ref. [4], Λ, the QCD dimensional parameter and Q_0 are independent of n, the order of the moments of the structure functions.

It is worth noting that $G_{\nu/P}$ in Eq. (9) is independent of Q^2 since the kinetic states of the valons in the proton should not depend on how much we can reveal of their components

with our probe. However, F^{ν} depends on Q^2, in analogous manner to the Q^2-dependent behavior of structure functions for hadrons.

We label the two valons in the proton with indices U for the u-type and D for the d-type valon. Thus, we can write the structure function of the U valon as

$$F_2^U(z,Q^2)=\frac{4}{9}z(G_{u/U}+G_{\bar{u}/U}) + \frac{1}{9}z(G_{d/U}+G_{\bar{d}/U}+G_{s/U}+G_{\bar{s}/U}), \quad (10)$$

where all the functions on the right-hand side are the probability functions for quarks having momentum fraction z in the U valon at Q^2. Similarly, for the D valon, we have

$$F_2^D(z,Q^2)=\frac{4}{9}z(G_{u/D}+G_{\bar{u}/D}) + \frac{1}{9}z(G_{d/D}+G_{\bar{d}/D}+G_{s/D}+G_{\bar{s}/D}). \quad (11)$$

Applying Eq. (1), the above expression becomes

$$F_2^U(z,Q^2)=\frac{4}{9}z[pG_f(z,Q^2)+(1-p)G_{uf}(z,Q^2) + 2qG_{uf}(z,Q^2) + 2(1-q)G_f(z,Q^2)], \quad (12)$$

$$F_2^D(z,Q^2)=\frac{1}{9}z[pG_f(z,Q^2)+(1-p)G_{uf}(z,Q^2) + 11qG_{uf}(z,Q^2) + 11(1-q)G_f(z,Q^2)]. \quad (13)$$

The flavor-singlet (S) and flavor-nonsinglet (NS) G functions are defined as

$$G^S(z,Q^2)=G_f(z,Q^2)+(2n_f-1)G_{uf}(z,Q^2), \quad (14)$$

$$G^{NS}(z,Q^2)=G_f(z,Q^2)-G_{uf}(z,Q^2), \quad (15)$$

where n_f is the number of quark flavors.

It is important to note that unlike Ref. [4], we do not denote $G^S(z,Q^2)$ and $G^{NS}(z,Q^2)$ as summations of the probability functions of the quarks and antiquarks present with respect to the all valons present. However, we have adhered to the usual definition of flavor singlet and nonsinglet in perturbative QCD [10] in Eqs. (14) and (15). Inverting, Eqs. (14) and (15) for G_f and G_{uf}, we get

$$G_f(z,Q^2)=\frac{1}{2n_f}[G^S(z,Q^2)+(2n_f-1)G^{NS}(z,Q^2)], \quad (16)$$

$$G_{uf}(z,Q^2)=\frac{1}{2n_f}(G^S-G^{NS}). \quad (17)$$

Taking the number of flavors, n_f, to be 3 and applying Eqs. (16) and (17) to Eqs. (12) and (13), we obtain

$$F_2^U(z,Q^2)=\frac{2}{9}z[G^S(z,Q^2)+(3+2p-4q)G^{NS}(z,Q^2)], \quad (18)$$

$$F_2^D(z,Q^2)=\frac{1}{9}z[2G^S(z,Q^2)+(9+p-11q)G^{NS}(z,Q^2)]. \quad (19)$$

The relations between the functions and moments are

$$M_2(n,Q^2)=\int_0^1 z^{n-2}F_2(z,Q^2)dz, \quad (20)$$

$$M^{\alpha}(n,Q^2)=\int_0^1 z^{n-1}G^{\alpha}(z,Q^2)dz, \quad (21)$$

where α denotes either a singlet S or nonsinglet NS-type valon within the proton, i.e., ν/P. Making use of Eq. (9), the moment of the proton structure function is

$$M_2^P(n,Q^2)=\sum_{\nu} M_{\nu/P}(n)M_2^{\nu}(n,Q^2)=2M_{U/P}(n)M_2^U(n,Q^2)+M_{D/P}(n)M_2^D(n,Q^2)$$

$$=2U^P(n)\int_0^1 z^{n-2}F_2^U(z,Q^2)dz+D^P(n)\int_0^1 z^{n-2}F_2^D(z,Q^2)$$

$$=\frac{2}{9}(2U^P+D^P)M^S+\frac{1}{9}[4U^P(3+2p-4q)+D^P(9+p-11q)]M^{NS}, \quad (22)$$

where we have replaced $M_{U/P}(n)$, the *u*-type valon distribution moment, by $U^P(n)$ and $M_{D/P}(n)$, the *d*-type valon distribution momentum, by $D^P(n)$.

Adopting the methods in Ref. [4], we have

$$U(n)=\frac{B(a+n,a+b+2)}{B(a+1,a+b+2)}, \tag{23}$$

$$D(n)=\frac{B(b+n,2a+2)}{B(b+1,2a+2)}, \tag{24}$$

where $B(m,n)$ is the Euler beta function with parameters *m* and *n*, and *a*, *b* are free parameters used to describe the exclusive valon distributions. Furthermore,

$$M^{NS}(n,Q^2)=\exp(-d_{NS}s), \tag{25}$$

$$M^{S}(n,Q^2)=\frac{1}{2}(1+\rho)\exp(-d_{+}s)+\frac{1}{2}(1+\rho)\exp(-d_{-}s), \tag{26}$$

with

$$s=\ln\left[\frac{\ln(Q^2/\Lambda^2)}{\ln(Q_0^2/\Lambda^2)}\right]. \tag{27}$$

The anomalous dimensions and associated parameters are given as

$$\rho=(d_{NS}-d_{gg})/\delta,$$

$$\delta=d_{+}-d_{-}=[(d_{NS}-d_{gg})^2+4d_{gQ}d_{Qg}]^{1/2},$$

$$d_{NS}=\frac{1}{3\pi\tilde{n}_f}\left[1-\frac{2}{n(n+1)}+4\sum_{j=2}^{n}\frac{1}{j}\right],$$

$$d_{gQ}=\frac{-2}{3\pi\tilde{n}_f}\frac{2+n+n^2}{n(n^2-1)},$$

$$d_{Qg}=\frac{-n_f}{2\pi\tilde{n}_f}\frac{2+n+n^2}{n(n+1)(n+2)},$$

$$d_{gg}=\frac{-3}{\pi\tilde{n}_f}\left[-\frac{1}{12}+\frac{1}{n(n-1)}+\frac{1}{(n+1)(n+2)}-\frac{n_f}{18}-\sum_{j=2}^{n}\frac{1}{j}\right],$$

$$d_{+}=\frac{1}{2}[d_{NS}+d_{gg}+\delta],$$

$$d_{-}=\frac{1}{2}[d_{NS}+d_{gg}-\delta],$$

$$\tilde{n}_f=\frac{(33-2n_f)}{12\pi}. \tag{28}$$

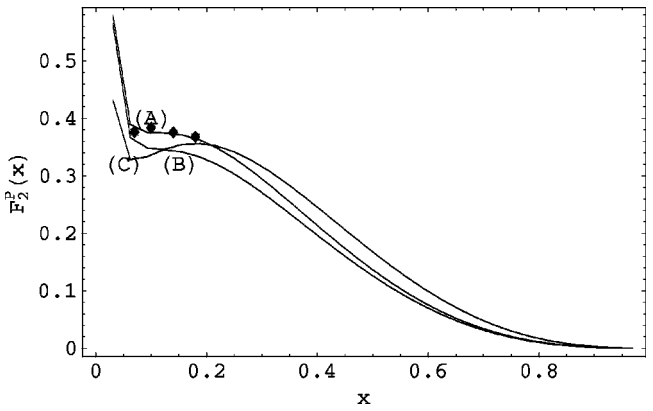

FIG. 1. Plots of proton structure function $F_2^p(x)$ versus *x* at $Q^2=8.75$ $(\mathrm{GeV/c^2})^2$. Curve (A) is plotted from the improved valon model with $p=0.95$, $q=0.95$. Curve (B) is plotted with $p=1$, $q=1$, which is the original valon model. Both are plotted with the best fit values of $Q_0=0.75$ GeV/c^2 and $\Lambda=0.65$ GeV/c^2. Curve (C) is plotted from the original valon model with $Q_0=0.8$ GeV/c^2 and $\Lambda=0.65$ GeV/c^2.

Substituting Eqs. (23)–(28) into Eq. (22), and applying the inverse Mellin transform of Eq. (7), the proton structure functions at particular values of Q^2 are evaluated with respect to *x*, the momentum fraction of the proton. As the values of $a=0.65$ and $b=0.35$ are Q^2 independent [4], we have adopted them here.

Figures 1, 2, and 3 show the comparisons between the original and improved valon models with experimental data [13,14] and the respective values of *p* and *q* are given. All the curves marked (A) in these figures match the experimental data better than when $p=1$ and $q=1$. The chosen values of Q_0 and Λ are the best fits. In contrast, the values from Ref. [4], $Q_0=0.8$ GeV/c^2 and $\Lambda=0.65$ GeV/c^2, do not fit as well. Furthermore, it can be observed that *p* and *q* approach unity when the Q^2 gets higher. This is compatible with our probabilistic approach of the classification of fa-

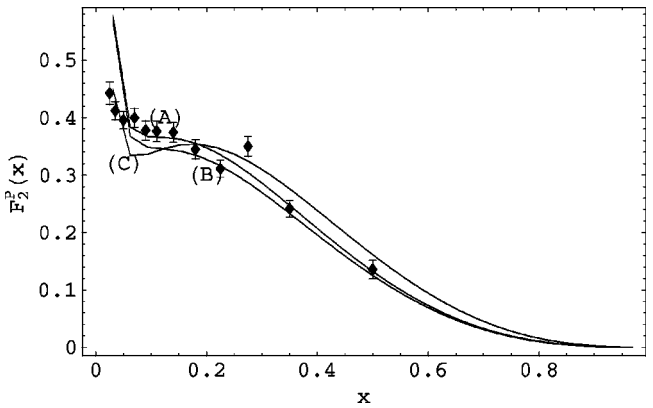

FIG. 2. Plots of proton structure function $F_2^p(x)$ versus *x* at $Q^2=9$ $(\mathrm{GeV}/c^2)^2$. Curve (A) is plotted from the improved valon model with $p=0.96$, $q=0.96$. Curve (B) is plotted with $p=1$, $q=1$, which is the original valon model. Both are plotted with the best fit values of $Q_0=0.75$ GeV/c^2 and $\Lambda=0.65$ GeV/c^2. Curve (C) is plotted from the original valon model with $Q_0=0.8$ GeV/ c^2 and $\Lambda=0.65$ GeV/c^2.

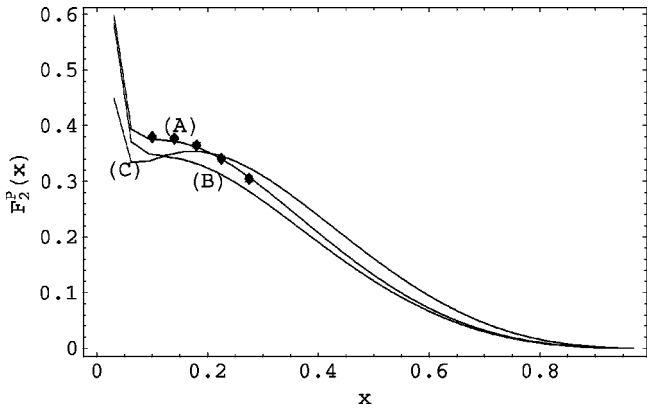

FIG. 3. Plots of proton structure functions $F_2^p(x)$ against x at $Q^2=10.25$ $(\mathrm{GeV/c^2})^2$. Curve (A) is plotted from the improved valon model with $p=0.96, q=0.96$. Curve (B) is plotted with $p=1$, $q=1$, which is the original valon model. Both are plotted with the best fit values of $Q_0=0.75$ GeV/c^2 and $\Lambda=0.65$ GeV/c^2. Curve (C) is plotted from the original valon model with $Q_0=0.8$ GeV/c^2 and $\Lambda=0.65$ GeV/c^2.

vored and unfavored distributions.

The fact that our fittings give better agreement at low Q^2 values speaks well for the validity of the improved valon model. Thus, it is reasonable to state that our present improved valon model constitues a good modification of the original valon model in the regime of low Q^2 [4].

V. PION TOTAL STRUCTURE FUNCTION MOMENTS

Describing the $\bar{u}$-type valon in terms of its parton distribution functions,

$$F_{\pi^-}^{\bar{U}}=z(G_{u/\bar{U}}+G_{\bar{u}/\bar{U}}+G_{d/\bar{U}}+G_{\bar{d}/\bar{U}}+G_{s/\bar{U}}+G_{\bar{s}/\bar{U}}). \tag{29}$$

Redefining $G_{\bar{u}/\bar{U}}$ as $\kappa G_f+(1-\kappa)G_{uf}$ while the other distributions as $\eta G_{uf}+(1-\eta)G_f$ as in Eq. (1) with κ and η being the respective weights, Eq. (29) thus becomes

$$F_{\pi^-}^{\bar{U}}=z[(5-5\eta+\kappa)G_f+(1+5\eta-\kappa)G_{uf}]. \tag{30}$$

A similar expression for d-type valons with weights $\hat{\eta}$ and $\hat{\kappa}$ is

$$F_{\pi^-}^{D}=z[(5-5\hat{\eta}+\hat{\kappa})G_f+(1+5\hat{\eta}-\hat{\kappa})G_{uf}]. \tag{31}$$

The total structure function moment is

$$\begin{aligned}M_{\mathrm{total}}^{\pi^-}&=M_{\bar{U}/\pi^-}\int_0^1 z^{n-2}F_{\pi^-}^{\bar{U}}(z,Q^2)dz\\&\quad+M_{D/\pi^-}\int_0^1 z^{n-2}F_{\pi^-}^{D}(z,Q^2)dz\\&=(\bar{U}^{\pi^-}+D^{\pi^-})M^S+[(4-5\eta+\kappa)\bar{U}^{\pi^-}\\&\quad+(4-5\hat{\eta}+\hat{\kappa})D^{\pi^-}]M^{NS},\end{aligned} \tag{32}$$

where we have defined the valon distributions

$$\bar{U}^{\pi^-}=M_{\bar{U}/\pi^-}, \tag{33}$$

$$D^{\pi^-}=M_{D/\pi^-}. \tag{34}$$

VI. PION VALENCE STRUCTURE FUNCTION MOMENTS

The π^- has two valence quarks: $\bar{u}_{valence}$ and $d_{valence}$ quarks. We define

$$\begin{aligned}\bar{u}&=\bar{u}_{valence}+\bar{u}_{sea},\\d&=d_{valence}+d_{sea}.\end{aligned} \tag{35}$$

From Eq. (9) and Ref. [15], the structure function of the $\bar{u}_{valence}$ quark can be written as

$$\begin{aligned}\bar{u}_{valence}(x,Q^2)&=\int_x^1\left[G_{\bar{U}/\pi^-}(y)G_{\bar{u}_{valence}/\bar{U}}\left(\frac{x}{y},Q^2\right)\right.\\&\quad\left.+G_{D/\pi^-}(y)G_{\bar{u}_{valence}/D}\left(\frac{x}{y},Q^2\right)\right]\frac{dy}{y}.\end{aligned} \tag{36}$$

A similar expression can also be derived for the d quark. The moment for the valence $\bar{u}$ quark is written as

$$\begin{aligned}M_{\bar{u}_{valence}}(n,Q^2)&=M_{\bar{U}/\pi^-}(n)M_{\bar{u}_{valence}/\bar{U}}(n,Q^2)+M_{D/\pi^-}(n)M_{\bar{u}_{valence}/D}(n,Q^2)\\&=\bar{U}^{\pi^-}(n)\int_0^1 x^{n-1}G_{\bar{u}_{valence}/\bar{U}}(x,Q^2)dx+D^{\pi^-}(n)\int_0^1 x^{n-1}G_{\bar{u}_{valence}/D}(z,Q^2)\\&=\bar{U}^{\pi^-}(n)\int_0^1 x^{n-1}[\zeta G_f+(1-\zeta)G_{uf}](x,Q^2)dx+D^{\pi^-}(n)\int_0^1 x^{n-1}[\varphi G_{uf}+(1-\varphi)G_f](z,Q^2)dx\\&=\frac{1}{6}\{(\bar{U}^{\pi^-}+D^{\pi^-})M^S+[(6\zeta-1)\bar{U}^{\pi^-}+(5-6\varphi)D^{\pi^-}]M^{NS}\},\end{aligned} \tag{37}$$

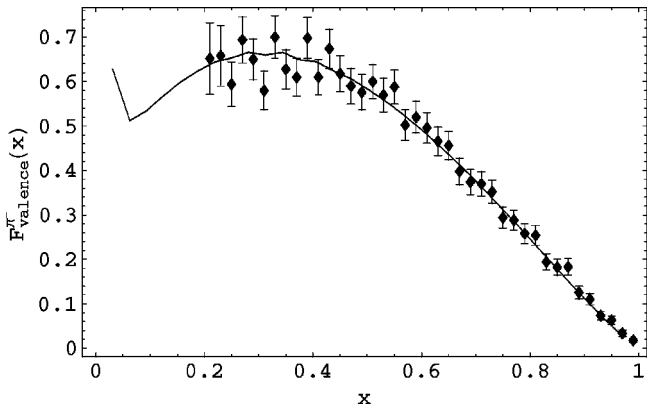

FIG. 4. Comparison of the pion valence structure function $F^{\pi^-}_{valence}(x)$ result from the improved valon model to data from E615 [16] at $Q^2=25$ $(\mathrm{GeV/c^2})^2$.

where we have done the replacement

$$G^{-}_{u_{valence}/\bar{U}}(x,Q^2)=[\zeta G_f+(1-\zeta)G_{uf}](x,Q^2),$$

$$G^{-}_{u_{valence}/D}(z,Q^2)=[\varphi G_{uf}+(1-\varphi)G_f](z,Q^2), \tag{38}$$

where, as in Eq. (1), ζ and φ refer to the respective weights or probabilities for the case of the valence distribution function. Since $M^{-}_{u_{valence}}=M_{d_{valence}}$, the following relation is the result:

$$M^{\pi^-}_{valence}(n,Q^2)=2M^{-}_{u_{valence}}(n,Q^2). \tag{39}$$

VII. VALON DISTRIBUTIONS

We assume a simple form for the exclusive valon distribution

$$G_{\bar{U}D/\pi^-}(y_1,y_2)=\alpha y_1^{\epsilon}y_2^{\tau}\delta(y_1+y_2-1), \tag{40}$$

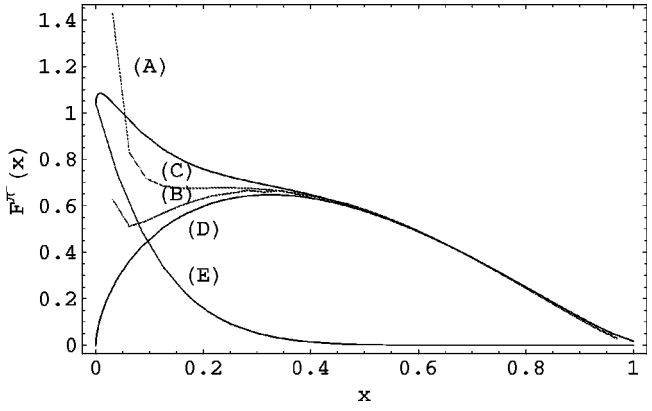

FIG. 5. Comparison of the pion structure functions $F^{\pi^-}(x)$. (A) and (B) are the total and valence structure functions from the improved valon model, respectively. (C), (D), and (E) are the total, valence, and sea structure functions from the parametrizations of E615 [16], respectively.

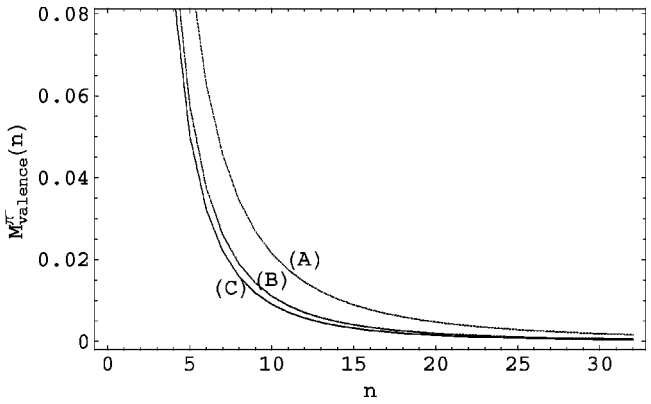

FIG. 6. Moments of valence structure functions $M^{\pi^-}_{valence}(n)$ plotted against order n. (A) is plotted at $Q^2=4.84$ $(\mathrm{GeV/c^2})^2$, (B) at 25 $(\mathrm{GeV/c^2})^2$, and (C) at 49 $(\mathrm{GeV/c^2})^2$.

where ϵ and τ are two Q^2-independent free parameters, similar to a and b in the case of proton, y_1 is the momentum fraction of the $\bar{u}$-type valon, and y_2 belongs to the d-type valon. The inclusive valon distributions can then be obtained through the relations

$$G_{\bar{U}/\pi^-}(y)=\int_0^1 G_{\bar{U}D/\pi}(y,y_2)dy_2$$
$$=y^{\epsilon}(1-y)^{\tau}B(\epsilon+1,\tau+1)^{-1}, \tag{41}$$

$$G_{D/\pi^-}(y)=\int_0^1 G_{\bar{U}D/\pi}(y_1,y)dy_1$$
$$=y^{\tau}(1-y)^{\epsilon}B(\tau+1,\epsilon+1)^{-1}. \tag{42}$$

Using conservation of momentum, one can determine α from the following sum rules:

$$\int_0^1 G_{\bar{U}/\pi^-}(y_1)dy_1=1,$$

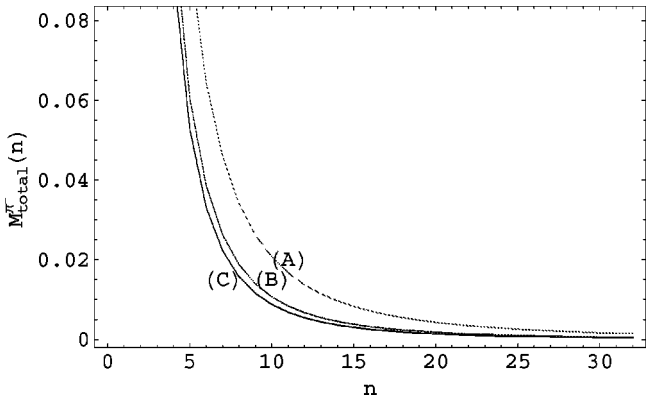

FIG. 7. Moments of the total structure functions $M^{\pi^-}_{total}(n)$ plotted against order n. (A) is plotted at $Q^2=4.84$ $(\mathrm{GeV/c^2})^2$, (B) at 25 $(\mathrm{GeV/c^2})^2$, and (C) at 49 $(\mathrm{GeV/c^2})^2$.

TABLE I. Calculated first and second moments of the total pion structure functions at $Q^2=4.84$ $(\mathrm{GeV/c^2})^2$, 25 $(\mathrm{GeV/c^2})^2$, and 49 $(\mathrm{GeV/c^2})^2$.

Moment	$Q^2=4.84$ $(\mathrm{GeV/c^2})^2$	25 $(\mathrm{GeV/c^2})^2$	49 $(\mathrm{GeV/c^2})^2$
First	0.58	0.52	0.50
Second	0.25	0.19	0.17

$$\int_0^1 G_{D/\pi^-}(y_2)dy_2=1. \tag{43}$$

A simple calculation yields the moments of the valon distribution functions as

$$\overline{U}^{\pi^-}(n)=\frac{B(\epsilon+n,\tau+1)}{B(\epsilon+1,\tau+1)},$$

$$D^{\pi^-}(n)=\frac{B(\tau+n,\epsilon+1)}{B(\tau+1,\epsilon+1)}. \tag{44}$$

Since the valon distribution functions are Q^2 independent, the free parameters ϵ and τ can be obtained phenomenologically using just inputs at one particular Q^2 value.

VIII. RELATING PION STRUCTURE FUNCTIONS TO EXPERIMENTAL DATA

We obtain the best fit values of $\epsilon,\tau,Q_0,\Lambda,\zeta,\varphi,\kappa,\eta,\hat{\kappa}$, and $\hat{\eta}$ by looking for a combination of ϵ and τ that produces the closest results to the parametrization of the E615 collaboration [16] for $x\geqslant 0.4$. Considerations are made for $Q_0=0.70$, 0.75, 0.80, 0.85, and 0.90 $\mathrm{GeV/c^2}$ and $\Lambda=0.50$, 0.55, 0.60, 0.65, and 0.70 $\mathrm{GeV/c^2}$. Equations (32), (37), and (39) and the inverse Mellin transform are used to obtain the structure function curves of every possible combination. Note that three sets of parameters $\{\zeta,\varphi\}$, $\{\kappa,\eta\}$, and $\{\hat{\kappa},\hat{\eta}\}$ are introduced to modify the favored and unfavored distributions for the valence quarks, the $\overline{U}$ valon, and the D valon, respectively. In each case, we assume a transformation of the form

$$G_f\rightarrow rG_f+(1-r)G_{uf},\quad G_{uf}\rightarrow sG_{uf}+(1-s)G_f,$$

where $\{r,s\}$ is the appropriate set of parameters. However, if we impose the additional condition that the total distribution, namely, G_f+G_{uf}, for each type of quark or valon remain unchanged in the process so that

TABLE II. Calculated first and second moments of the valence pion structure functions at $Q^2=4.84$ $(\mathrm{GeV/c^2})^2$, 25 $(\mathrm{GeV/c^2})^2$, and 49 $(\mathrm{GeV/c^2})^2$.

Moment	$Q^2=4.84$ $(\mathrm{GeV/c^2})^2$	25 $(\mathrm{GeV/c^2})^2$	49 $(\mathrm{GeV/c^2})^2$
First	0.56	0.47	0.44
Second	0.25	0.18	0.17

TABLE III. Comparisons of the calculated moments of total pion structure functions from our improved valon model with lattice QCD [20] calculations at $Q^2=4.84$ $(\mathrm{GeV/c^2})^2$.

Moment	First	Second
Lattice QCD	0.60 ± 0.08	0.23 ± 0.06
Improved valon model	0.58	0.25

$$G_f+G_{uf}\rightarrow(1-s+r)G_f+(1-r+s)G_{uf},$$

then we can equate the coefficients of the terms in G_f and G_{uf} to unity, giving $r=s$. Thus, by assuming the invariance of the total distribution, namely, favored and unfavored, for valence quarks, $\overline{U}$ valons, and D valons, we can eliminate some of the free parameters through the relations $\zeta=\varphi$, $\kappa=\eta$, and $\hat{\kappa}=\hat{\eta}$. Moreover, if we allow the values of ζ, κ, and $\hat{\kappa}$ to vary, we observe that the values of ζ, κ, and $\hat{\kappa}$ are approximately equal.[2] Consequently we may let $\zeta=\varphi=\kappa=\eta=\hat{\kappa}=\hat{\eta}$ and scan values of ζ with the values 0.90,0.95,0.98,1.0. The last case reduces to the original valon model.

The results are

$$\epsilon=0.01,$$

$$\tau=0.06,$$

$$Q_0=0.90\ \ \mathrm{GeV/c^2},$$

$$\Lambda=0.70\ \ \mathrm{GeV/c^2},$$

$$\zeta=\varphi=\kappa=\eta=\hat{\kappa}=\hat{\eta}=0.98. \tag{45}$$

Figure 4 shows the comparison between the valence structure function curve plotted from these results and the experimental data from the E615 collaboration [16] at $Q^2=25$ $(\mathrm{GeV/c^2})^2$. Comparison of total and valence structure functions with the theoretical parametrization of the E615 Collaboration [16] at $Q^2=25$ $(\mathrm{GeV/c^2})^2$ is also made and shown in Fig. 5.

Figures 6 and 7 show the moments calculated at $Q^2=4.84$, 25, and 49 $(\mathrm{GeV/c^2})^2$ for the valence and total pion structure functions, respectively. Tables I, II, III, and IV display our values for the first two moments of the total and valence structure functions as compared to other sources.

Our calculated moments and their structure functions appear to agree with the experimental data well. These results again testify the relevance of the physical idea behind the improved valon model.

[2]In earlier simulations, we perform an elaborate fitting of the model without this assumption. For those parameters that we have randomly attempted, our best fit values of $\zeta,\varphi,\kappa,\eta,\hat{\kappa}$, and $\hat{\eta}$ are found to be very closed to each other.

TABLE IV. Comparisons of the calculated moments of valence pion structure functions from our improved valon model with that from lattice QCD [20] and the Nambu–Jona-Lasinio model [21–23] calculations and experiment [17–19] data at $Q^2=49$ $(\mathrm{GeV/c^2})^2$.

Moment	First	Second
Lattice QCD	0.46 ± 0.07	0.18 ± 0.05
NJL model	0.41	0.16
Experiment	0.40 ± 0.02	0.16 ± 0.01
Improved valon model	0.44	0.17

IX. SCALE-BREAKING EFFECTS

We examine the scale-breaking effects of the pion total structure function. As scale breaking is expected to steepen the structure function at high x regions for the higher Q^2 data, the trends exhibited at high Q^2 values are specifically noted.

We would expect the free parameters κ, η, $\hat{\kappa}$, and $\hat{\eta}$ to be Q^2 dependent, though we do not know how they vary with Q^2 without new experimental data. However, if we assume on the contrary that these parameters are Q^2 independent, we can perform the simulations at various Q^2 and look at their variation in their structure functions. Figure 8 shows the total structure functions at different Q^2, with the Q^2 falling within the range of 4 $(\mathrm{GeV/c^2})^2$ and 500 $(\mathrm{GeV/c^2})^2$. At high Q^2, scale breaking is not observed and the difference between the structure functions diminishes.

X. CONCLUSIONS

In general, the valon model bridges the gap between the bound-state and scattering problems of the hadron. The original model has been shown to be successful in describing the structure functions of nucleons to the extent of setting up parametrizations of parton distributions. We have shown that the improved valon model can describe DIS data of proton at low Q^2 very well.

This improved valon model is also applied to Drell-Yan scattering, from which the structure functions of pion are estimated. Our fittings of the modified structure function equations to the existing data are good and the calculated first and second moments also compare favorably with some other theoretical calculations and experimental data.

We predict that the dip at around $x=0.05$ exists for the pion valence structure function at $Q^2=25$ $(\mathrm{GeV/c^2})^2$. This can only be verified after the DIS data for pions are available later this year. Last, we conduct an interesting examination on the scale-breaking property of this model under the assumption that our fitted quark distribution functions weights are Q^2 independent.

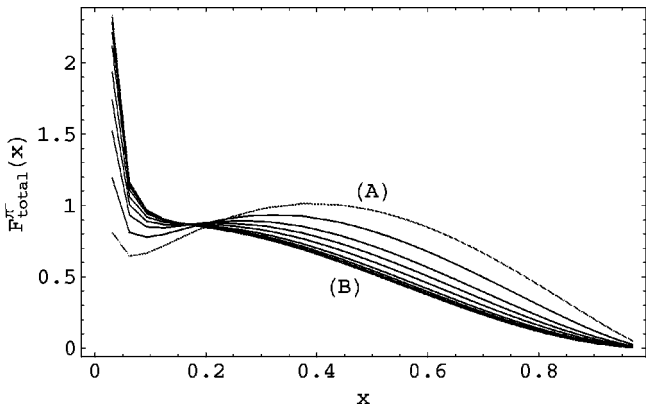

FIG. 8. Curves of pion total structure function $F^{\pi^-}_{total}(x)$ versus x. (A) is plotted at $Q^2=4$ $(\mathrm{GeV/c^2})^2$ and (B) at $Q^2=500$ $(\mathrm{GeV/c^2})^2$. The rest of the curves are $Q^2=10$, 25, 50, 100, 200, 300, and 400 $(\mathrm{GeV/c^2})^2$. The higher the Q^2 of a curve, the closer it is to (B).

[1] G. Altarelli, N. Cabibbo, L. Maiani, and R. Petronzio, Nucl. Phys. **B69**, 531 (1974); N. Cabibbo and R. Petronzio, *ibid.* **B137**, 395 (1978).

[2] R. C. Hwa, Phys. Rev. D **22**, 759 (1980).

[3] R. C. Hwa, Phys. Rev. D **22**, 1593 (1980).

[4] R. C. Hwa and M. S. Zahir, Phys. Rev. D **23**, 2539 (1981).

[5] T. T. Chou and C. N. Yang, in *High Energy Physics and Nuclear Structure*, edited by G. Alexander (North-Holland, Amsterdam, 1967), p. 348; Phys. Rev. **170**, 1591 (1968).

[6] Firooz Arash, Phys. Rev. D **50**, 1946 (1994).

[7] J. Ashman *et al.*, Phys. Lett. B **206**, 364 (1988); Nucl. Phys. **B328**, 1 (1989).

[8] C. Fuglesang, in *Proceedings of the XIX International Symposium on Multiparticle Dynamics* (World Scientific, Singapore, 1988), p. 257.

[9] F. J. Yndurain, Phys. Lett. **74B**, 68 (1978).

[10] Thomas Degrand, Nucl. Phys. **B151**, 485 (1979).

[11] C. Lopez and F. J. Yndurian, in *Pade Approximants and Their Applications*, edited by P. Graves-Morris (Academic, New York, 1973), and work quoted therein.

[12] J. A. Shohart and J. D. Tamarkin, *The Problem of Moments* (American Mathematical Society, New York, 1943).

[13] New Muon Collaboration (NMC), M. Arneodo *et al.*, Phys. Lett. B **364**, 107 (1995).

[14] BCDMS Collaboration, A. C. Benvenuti *et al.*, Phys. Lett. B **223**, 485 (1989).

[15] G. Altarelli, S. Petrarca, and F. Rapuano, Phys. Lett. B **373**, 200 (1996).

[16] J. S. Conway *et al.*, Phys. Rev. D **39**, 92 (1989).

[17] P. J. Sutton, A. D. Martin, R. G. Roberts, and W. J. Stirling, Phys. Rev. D **45**, 2349 (1992).

[18] B. Betev *et al.*, Z. Phys. C **28**, 9 (1985); B. Betev *et al.*, *ibid.* **28**, 15 (1985); B. Mours, Ph. D. thesis, L'Universite Louis Pasteur de Strasbourg, 1984.

[19] J. Badier *et al.*, Z. Phys. C **18**, 281 (1983).

[20] G. Martinelli and C. T. Sachrajda, Nucl. Phys. **B306**, 865 (1988).

[21] T. Shigetani, K. Suzuki, and H. Toki, Phys. Lett. B **308**, 383 (1993).

[22] C. L. Korpa and U. G. Meissner, Phys. Rev. D **41**, 1679 (1990).

[23] M. Burkardt and B. J. Warr, Phys. Rev. D **45**, 958 (1992).